Polymer Chemistry

Accepted Manuscript

ROYAL SOCIETY OF CHEMISTRY

www.rsc.org/polymers

Polymer Chemistry

PAPER

Ultrahighly Electron-Deficient Pyrrolo-acenaphtho-pyridazine-dione Based Donor-Acceptor Conjugated Polymers for Electrochromic Applications

Received 00th January 20xx,
Accepted 00th January 20xx

DOI: 10.1039/x0xx00000x

www.rsc.org/

Ching Mui Cho,[a,b,†] Qun Ye,[a,†] Wei Teng Neo,[a,c] Tingting Lin,[a] Xuehong Lu,[b,*] and Jianwei Xu [a,d,*]

Novel electron acceptors 2-alkyl-6,9-di(thiophen-2-yl)-1*H*-pyridazino[4',5':2,3]indeno[6,7,1-*def*]isoquinoline-1,3(2*H*)-dione and 2-alkyl-6,9-di(furan-2-yl)-1*H*-pyridazino[4',5':2,3]indeno[6,7,1-*def*]isoquinoline-1,3(2*H*)-dione derived from pyrrolo-acenaphtho-pyridazine-dione (PAPD) with a very low-lying lowest unoccupied molecular orbital (LUMO) level have been synthesized *via* a regioselective inverse electron demand Diels-Alder reaction between thiophene- and furan-substituted 1,2,4,5-tetrazine and an electron-deficient compound 2-(2-alkyl)-1*H*-indeno[6,7,1-*def*]isoquinoline-1,3(2*H*)-dione. The chemical structures of two PAPD monomers were confirmed by ^{1}H and ^{13}C nuclear magnetic resonance (NMR) spectroscopy, mass spectrometry as well as single-crystal X-ray structural analysis. The time-dependent density functional theory (TD-DFT) calculations were performed to show that PAPD series monomers have a LUMO energy level of down to -3.42 eV, much lower than those popular electron acceptors such as benzotriazole, benzothiadiazole and its fluorinated derivative (-2.19 – -2.98 eV). The PAPD based monomer was incorporated into a series of donor-acceptor type conjugated polymers comprising 3,3-bis((dodecyloxy)methyl)-3,4-dihydro-2*H*-thieno[3,4-*b*][1,4]dioxepine and thieno[3,2-*b*]thiophene as co-monomers through Stille coupling polymerization to give electrochromic conjugated polymers **P1** – **P5** with high number-molecular weights in the range of 42,000 – 67,000 (g/mol). The polymers showed optical bandgaps between 1.90 – 1.99 eV. Electrochromic devices displayed reversible color changes between purple/red at neutral state and greyish blue/grey at oxidized state with outstanding redox stability of less than 1 % decrease in contrast after 800 cycles using polymer **P3** as an example, and high optical contrasts of up to 80 % at 1500 nm in the near infrared region.

1. Introduction

In recent years, conjugated polymers have gained popularity in the field of organic electronics including organic solar cells,[1] organic field-effect transistors,[2] organic light-emitting diodes[3] and organic electrochromic materials.[4] These organic electrochromic materials are favored over inorganic electrochromic materials as they have faster response speed,[5] exhibit higher optical contrasts in a wide range of color,[6] outstanding coloration efficiency[7] and the cost effectiveness[8] for large scale production. As such, conjugated polymer based organic electrochromic materials are excellent candidates in a wide range of applications such as smart windows,[9] electrochromic displays,[10] and electrochromic inks.[11]

Great efforts have been made to develop novel electrochromic conjugated polymers that deliver high performance, and one of the most effective methodologies is through the donor-acceptor (DA) approach. The DA approach is to create low bandgap polymers[12] consisting of alternating electron donors and acceptors. This works by means of tuning the highest occupied molecular orbital (HOMO) and the lowest unoccupied molecular orbital (LUMO) energy levels. Typically, DA conjugated polymers have the characteristic dual absorption peaks[13] which aid color-tuning, especially for green[14] and black[10,15] polymers at the neutral state. In addition, it was widely reported that DA conjugated polymers gave good electrochromic performance which could be attributed to the increased intramolecular interactions for efficient charge transport.[16] Electrochromic properties such as stability, coloration efficiency, switching speed and optical contrast were thus greatly improved.

As an ongoing effort to prepare conjugated polymers for high performance electrochromic materials, it is particularly of interest in the design and development of new electron deficient monomers for DA type conjugated polymers. From our previous work, we have discovered a synthesis method that relies on the inverse electron demand Diels-Alder reaction between aryl-substituted tetrazine and dienophiles.[17] By adopting this novel synthesis methodology, we have developed new ultrahighly electron deficient monomers, pyrrolo-acenaphtho-pyridazine-dione (PAPD). There are two attributes of this new type of electron acceptors that need to be

[a] *Institute of Materials Research and Engineering, Agency for Science, Technology and Research (A*STAR), 3 Research Link, Singapore, 117602*
Email: jw-xu@imre.a-star.edu.sg
[b] *School of Materials Science and Engineering, Nanyang Technological University, 50 Nanyang Avenue, Singapore 639798.*
Email: ASXHLu@ntu.edu.sg
[c] *NUS Graduate School for Integrative Sciences and Engineering, National University of Singapore, 28 Medical Drive, Singapore 117456*
[d] *Department of Chemistry, National University of Singapore, 3 Science Drive 3, Singapore 117543*
† *These two authors contribute equally to this work.*
Electronic Supplementary Information (ESI) available: Characterization data of all new compounds; DFT calculation details; X-ray crystallographic data and more electrochromic characterization data. See DOI: 10.1039/x0xx00000x

highlighted. Firstly, these new monomers possess an ultrahigh electron deficiency owning to the combination of strong electron-withdrawing imide group, five-membered ring and pyridazine moiety which are of great importance to fine-tune the physical properties of the DA type conjugated polymers, such as the bandgap, color, and frontier orbital energy levels. Introduction of ultra-highly electron-deficient monomers into the electrochromic materials aims to control the frontier orbital of the final polymers. Poly(ethylenedioxythiophene) (PEDOT) and related derivative polymers have superior performance for electrochromic applications, but their ambient stability is limited by their relatively high-lying HOMO energy level. In order to stabilize these polymers, electron deficient acceptors are commonly introduced into the polymer backbone to lower the HOMO energy level. We compared the LUMO energy level of the PAPD unit with some of those commonly used electron acceptors by means of time-dependent density functional theory (TD-DFT) calculations (Figure 1). Out of these electron acceptors, the PAPD possesses the lowest LUMO energy level with -3.42 eV, much lower than these frequently used benzotriazole and benzothiadiazole based electron acceptors. Also, the ultra-highly electron-deficient monomers could be used to tune the absorption and the neutral color of the donor-acceptor conjugated polymers. Secondly, the PAPD monomer possesses the convenience of side chain engineering at the imide-N position and allows it to be easily incorporated into polymeric structures by conventional palladium catalyzed cross-coupling polymerization reactions. In this paper, we demonstrated the synthesis and characterization of a series of high performance electrochromic DA conjugated polymers with a new PAPD monomer.

2. Experimental Section

2.1 Materials

All reagents and starting materials were purchased from commercial sources and used without further purification unless otherwise stated.

2.2 Instrumentation

^{1}H NMR and ^{13}C NMR spectra were obtained in $CDCl_3$ on Avance 400 MHz Bruker spectrometer. HR-EI-MS was carried out on Finnigan TSQ 7000 triple stage quadrupole mass spectrometer. UV-*vis*/UV-*vis*-NIR absorption spectra were obtained with a Shimadzu UV 3600 UV-*vis*-NIR spectrophotometer. All chemical shifts are quoted in ppm, relative to tetramethylsilane, using the residual solvent peak as a reference standard. Polymer molecular weights were determined using an Alliance Waters model 2690 gel permeation chromatography (GPC) system calibrated with polystyrene (PS) as the standard and THF as the eluent. Polymer of 5 mg/mL concentration was prepared and filtered prior to sample injection. Elemental analysis data were acquired on a Flash EA 1112 series. The thermogravimetric analysis of the polymers was performed on a Perkin Elmer TGA-7 thermal analyzer under nitrogen at a heating rate of 20 ^{o}C/min. Differential scanning calorimetry (DSC) measurements were carried out using a PDSC Q100 from TA instruments with a heat-cool profile from -40 ^{o}C to 200 ^{o}C at a rate of 10 ^{o}C min^{-1} for three cycles under a constant N_2 flow. Cyclic voltammetry and chronoamperometry experiments were carried out using an Autolab PGSTAT128N potentiostat. Colourimetry data was acquired using Hunterlab ColorQuest XE and the colour of each polymer film was assessed by utilizing the CIE 1976 L*a*b* colour space with a D65/10^{o} illuminant. X-ray diffraction (XRD) patterns of the thin films were recorded using a Cu-Kα radiation source (λ = 0.15406 nm) on a Shimadzu XRD-6000. X-ray crystal structure determination was performed on a Bruker X8 Diffractometer. The structures were solved by direct methods with any remaining non-hydrogen atoms located from different Fourier maps. All non-hydrogen atoms were refined anisotropically. Hydrogen atoms were placed in calculated positions with fixed isotropic thermal parameters. Refinements were made by full-matrix least-squares methods and final refinements were made on F2 using a weighting scheme of the form $w = 1/[\sigma^2(F_0^2 + (aP)^2 + bP]$, where $P = [\max(F_0^2) + 2(F_c^2)]/3$.

2.3 Cyclic Voltammetry and Spectroelectrochemistry

For cyclic voltammetry, measurements were done in a MBraunLABmaster 130 glove box. The solutions of **P1 – P5** in chlorobenzene (10 mg/mL) were drop casted onto glassy carbon electrode. A three electrode cell configuration with polymer-coated glassy carbon, Pt wire and Ag wire as the working, counter, and pseudo-reference electrodes respectively was employed. A 0.1 M $LiClO_4$/ACN electrolyte/solvent couple was used and all measurements were recorded at 50 mV/s. The pseudo-reference electrode was calibrated against the ferrocene/ferrocenium redox couple. For spectroelectrochemical studies, the polymers were analyzed in their device forms.

2.4 Device Fabrication

Electrochromic layers of **P1 – P5** on ITO/glass were deposited by a drop-and-spread method. The gel electrolyte was prepared by mixing 0.512 g of lithium perchlorate and 2.8 g of poly(methyl methacrylate) of molecular weight 120 kg/mol in 6.65 mL of propylene carbonate and 28 mL of dry acetonitrile (ACN). A window-type absorption/transmission electrochromic device (ECD) was constructed, with the sandwich structure Glass/ITO|polymer||electrolyte||ITO/Glass. Parafilm was used as the spacer to prevent electrical contact between the substrates.

2.5 Synthesis

2-(2-Octyldodecyl)-1*H*-indeno[6,7,1-*def*]isoquinoline-1,3(2*H*)-dione (6) To a dry round bottom flask was added 2-(2-octyldodecyl)-6,7-dihydro-1*H*-indeno[6,7,1-def]isoquinoline-1,3(2*H*)-dione (0.50 mmol), N-bromosuccinimide (0.55 mmol), benzoyl peroxide (0.05mmol) and dichloroethane (10 mL). The mixture was purged with argon for 15 min and then refluxed overnight. The precipitate was directly removed by filtration and

the resultant filtrate was rotary evaporated to dryness. The crude product was used without further purification. A solution of the above crude product (0.40 mmol), LiBr (1.2 mmol) and dry N,N-dimethylformamide (DMF) (10 mL) was heated at 115 ^{o}C for 2 hours. After cooling to room temperature, the solvent was removed by rotary evaporation and the residue was directly subjected to silica gel column chromatography using eluent (hexane : $CHCl_3$ = 3 : 1) to afford the target compound. Yield: 63%. ^{1}H NMR (400 MHz, $CDCl_3$): δ (ppm) 8.33 – 8.31 (d, 2H, *J* = 6.8 Hz), 7.72 – 7.70 (d, 2H, *J* = 6.8 Hz), 7.07 (s, 2H), 4.08 – 4.06 (d, 2H, *J* = 7.2 Hz), 1.96 – 1.94 (m, 1H), 1.39 – 1.21 (m, 32H), 0.88 – 0.83 (m, 6H). ^{13}C NMR (100 MHz, $CDCl_3$): δ (ppm) 164.7, 144.7, 133.3, 132.1, 127.9, 125.4, 123.7, 123.3, 44.8, 37.3, 32.3, 32.1, 30.4, 30.0, 29.7, 26.9, 23.1, 14.5. HR-EI-MS: *m/z* = 501.36086, calculated exact mass: 501.36013, error: 1.44 ppm.

6,9-Bis(5-bromothiophen-2-yl)-2-(2-octyldodecyl)-1*H*-pyridazino[4',5':2,3]indeno[6,7,1-*def*]isoquinoline-1,3(2*H*)-dione (10) To a dry round bottom flask was added 3,6-bis(5-bromothiophen-2-yl)-1,2,4,5-tetrazine **(8)** (0.50 mmol), 2-(2-octyldodecyl)-1*H*-indeno[6,7,1-*def*]isoquinoline-1,3(2*H*)-dione **(6)** (0.50 mmol) and diphenyl ether (10 mL). The mixture was purged with argon for 15 min and then heated to 160 ^{o}C overnight. After cooling to room temperature, the mixture was directly subjected to silica gel column chromatography. Hexane was used first to flush away the diphenyl ether and the target compound was then collected as red solid using eluent (hexane : $CHCl_3$ = 1 : 2). Yield: 40%. ^{1}H NMR (400 MHz, $CDCl_3$): δ (ppm) 8.49 – 8.44 (m, 4H), 7.62 – 7.61 (d, 2H, *J* = 4.0 Hz), 7.29 – 7.28 (d, 2H, *J* = 3.6 Hz), 4.05 – 4.03 (d, 2H, *J* = 7.2 Hz)), 1.93 (m, 1H), 1.37 – 1.20 (m, 32H), 0.86 – 0.82 (m, 6H). ^{13}C NMR (100 MHz, $CDCl_3$): δ (ppm) 163.6, 150.2, 140.4, 137.7, 133.5, 132.3, 131.0, 129.7, 127.1, 125.7 118.1, 45.1, 37.2, 32.3, 32.1, 30.4, 30.0, 29.72, 29.70, 26.9, 23.1, 14.5. HR-EI-MS: *m/z* = 873.16315, calculated exact mass: 873.16275, error: 0.46 ppm.

6,9-Bis(5-bromothiophen-2-yl)-2-hexyl-1*H*-pyridazino[4',5':2,3]indeno[6,7,1-*def*]isoquinoline-1,3(2*H*)-dione (11) To a dry round bottom flask was added 3,6-bis(5-bromothiophen-2-yl)-1,2,4,5-tetrazine **(8)** (0.50 mmol), 2-hexyl-1*H*-indeno[6,7,1-*def*]isoquinoline-1,3(2*H*)-dione **(7)** (0.50 mmol) and diphenyl ether (10 mL). The mixture was purged with argon for 15 min and then heated to 160 ^{o}C overnight. After cooling to room temperature, the mixture was directly subjected to silica gel column chromatography. Hexane was used first to flush away the diphenyl ether and the target compound was then collected as red solid using eluent (hexane : $CHCl_3$ = 1 : 2). Yield: 42%. ^{1}H NMR (400 MHz, $CDCl_3$): δ (ppm) 8.51 – 8.45 (m, 4H), 7.63 – 7.62 (d, 2H, *J* = 3.2 Hz), 7.30 – 7.29 (d, 2H, *J* = 2.8 Hz), 4.15 – 4.11 (t, 2H, *J* = 7.6 Hz), 1.89 (m, 2H), 1.74 – 1.67 (m, 2H), 1.42 – 1.32 (m, 4H), 0.90 – 0.87 (t, 3H, *J* = 6.8 Hz). ^{13}C NMR (100 MHz, $CDCl_3$): δ (ppm) 163.2, 150.2, 140.4, 137.8, 133.5, 132.2, 131.0, 129.7, 127.1, 125.8, 125.6, 118.1, 41.1, 31.9, 28.7, 27.2, 22.9, 14.4. HR-EI-MS: *m/z* = 676.94481, calculated exact mass: 676.94364, error: 1.72 ppm.

6,9-Bis(5-bromofuran-2-yl)-2-hexyl-1*H*-pyridazino[4',5':2,3]indeno[6,7,1-*def*]isoquinoline-1,3(2*H*)-dione (12) To a dry round bottom flask was added 3,6-bis(5-bromofuran-2-yl)-1,2,4,5-tetrazine **(9)** (0.50 mmol), 2-hexyl-1*H*-indeno[6,7,1-*def*]isoquinoline-1,3(2*H*)-dione **(7)** (0.50 mmol) and diphenyl ether (10 mL). The mixture was purged with argon for 15 min and then heated to 160 ^{o}C overnight. After cooling to room temperature, the mixture was directly subjected to silica gel column chromatography. Hexane was used first to flush away the diphenyl ether and the target compound was then collected as red solid using eluent (hexane : $CHCl_3$ = 1 : 2). Yield: 38%. ^{1}H NMR (400 MHz, $CDCl_3$): δ (ppm) 8.87 – 8.85 (d, 2H, *J* = 7.6 Hz), 8.58 – 8.56 (d, 2H, *J* = 7.6 Hz), 7.60 – 7.59 (d, 2H, *J* = 3.2 Hz), 6.73 – 6.72 (d, 2H, *J* = 3.6 Hz), 4.20 – 4.16 (t, 2H, *J* = 7.6 Hz), 1.79 – 1.68 (m, 2H), 1.46 – 1.25 (m, 6H), 0.93 – 0.89 (t, 3H, *J* = 6.8 Hz). ^{13}C NMR (100 MHz, $CDCl_3$): δ (ppm) 163.2, 153.0, 144.7, 136.9, 132.0, 131.2, 130.8, 129.3, 125.1, 124.8, 116.4, 115.3, 41.1, 32.0, 28.7, 27.2, 23.0, 14.5. HR-EI-MS: *m/z* = 644.99016, calculated exact mass: 644.98933, error: 1.28 ppm.

General procedure for Stille cross-coupling polymerization 6,9-bis(5-bromothiophen-2-yl)-2-(2-octyldodecyl)-1*H*-pyridazino[4',5':2,3]indeno[6,7,1-*def*]isoquinoline-1,3(2*H*)-dione **(10)** (0.05 mmol), 6,8-dibromo-3,3-bis((dodecyloxy)methyl)-3,4-dihydro-2*H*-thieno[3,4-*b*][1,4]dioxepine **(13)** (0.45 mmol) and 2,5-bis(trimethylstannyl)thieno[3,2-*b*]thiophene **(14)** (0.50 mmol) were dissolved in 12 mL of toluene. The mixture was stirred and purged with argon for about 15 min, and then $Pd(PPh_3)_4$ (0.025 mmol) was added. The flask was purged with argon for another 15 min before the mixture was heated to 110 ^{o}C for 48 hrs. After cooling to room temperature, the solvent was removed under reduced pressure and the residue was precipitated in methanol. The suspension was filtered to give the crude product, which was then purified by Soxhlet extraction with acetone, hexane and chloroform. The chloroform fraction was evaporated to dryness to afford dark red solid.

P1: Yield 55%. ^{1}H NMR (main signals) (400 MHz, $CDCl_3$): δ (ppm) 7.36 – 7.30 (br, m), 4.35 – 4.05 (br, m), 3.61 – 3.46 (br, m), 1.56 – 1.26 (br, m), 0.88 (br, s). Anal. Calcd for $C_{39}H_{60}O_4S_3$: C, 67.97; H, 8.78; S, 13.96. Found: C, 67.91; H, 8.79; S, 13.99. GPC using PS in THF as standard: Number-average molecular weight (M_n) = 50.5 k, Weight-average molecular (M_w) = 94.2 k, polydispersity index (PDI) = 1.86.

P2: Yield 55%. ^{1}H NMR (main signals) (400 MHz, $CDCl_3$): δ (ppm) 8.44 – 6.87 (br, m), 4.22 – 4.06 (br, m), 3.60 – 3.45 (br, m), 2.04 (br, s), 1.67 – 1.58 (br, m), 0.87 – 0.71 (br, m). Anal. Calcd for $C_{40.1}H_{59.1}N_{0.3}O_{3.8}S_{3.1}$: C, 68.26; H, 8.44; N, 0.59; S, 14.09. Found: C, 68.07; H, 8.45; N, 0.54; S, 14.01. GPC using PS in THF as standard: (M_n = 42.1 k, M_w = 83.5 k, PDI = 1.98)

P3: Yield 50%. ^{1}H NMR (main signals) (400 MHz, $CDCl_3$): δ (ppm) 8.48 – 6.87 (br, m), 4.21 – 4.04 (br, m), 3.60 – 3.44 (br, m), 2.04 (br, s), 1.68 – 1.59 (br, m), 0.87 (br, s). Anal. Calcd for $C_{41.2}H_{58.2}N_{0.6}O_{3.6}S_{3.2}$: C, 68.52; H, 8.12; N, 1.16; S, 14.21. Found: C, 67.97; H, 8.16; N, 0.99; S, 14.08. GPC using PS in THF as standard: (M_n = 48.3 k, M_w = 73.4 k, PDI = 1.52)

P4: Yield 54%. ^{1}H NMR (main signals) (400 MHz, $CDCl_3$): δ (ppm) 8.60 – 6.72 (br, m), 4.22 – 4.04 (br, m), 3.60 – 3.44 (br, m), 2.02 – 2.00 (br, m), 1.58 (br, s), 0.87 (br, s). Anal. Calcd for $C_{42.3}H_{57.3}N_{0.9}O_{3.4}S_{3.3}$: C, 68.78; H, 7.82; N, 1.71; S, 14.33. Found: C, 68.60; H, 7.83; N, 1.65; S, 14.28. GPC using PS in THF as standard: (M_n = 54.5 k, M_w = 93.8 k, PDI = 1.72)

P5: Yield 52%. ^{1}H NMR (main signals) (400 MHz, $CDCl_3$): δ (ppm) 8.52 – 6.88 (br, m), 4.22 – 4.07 (br, m), 3.59 – 3.44 (br, m), 2.13 – 2.01 (br, m), 1.57 – 0.86 (br, m). Anal. Calcd for $C_{46.7}H_{53.7}N_{2.1}O_{2.6}S_{3.7}$: C, 69.70; H, 6.73; N, 3.66; S, 14.74. Found: C, 69.29; H, 6.75; N, 3.52; S, 14.64. GPC using PS in THF as standard: (M_n = 67.2 k, M_w = 114.7 k, PDI = 1.71)

3. Results and Discussion

3.1 Synthesis and characterization

The synthesis of the PAPD monomers (**10** – **12**) is outlined in Scheme 1. Starting from the commercially available acenaphthene **1**, compounds **2** – **5** were synthesized *via* reported synthetic methods.[18] The subsequent bromination reaction with N-bromosuccinimide (NBS) in hot 1,2-dichloroethane, followed by an elimination process afforded dienophile intermediates 2-(2-alkyl)-1*H*-indeno[6,7,1-*def*]isoquinoline-1,3(2*H*)-diones **6** – **7**. Following our established methodology,[17] the inverse electron demand Diels-Alder reaction between compounds **6** – **7** as the dienophile moiety, and thiophene- and furan-substituted 1,2,4,5-tetrazine derivatives **8** – **9**[17,19] as the diene moiety in diphenyl ether occurred at 160 °C to afford monomers **10** – **12**. Similar to our previously reported, we observed the region-selective Diels-Alder reaction happened on the tetrazine moiety instead of on the thiophene or furan moiety. In order to understand why the Diels-Alder reaction only takes place on the central tetrazine unit, we calculated the activation energy ($\Delta G^{\neq}$) for the two possible reaction pathways between compounds **6** and **8** or **9,** and the results are summarized in Figure 2. To simplify the computation process, the branched substituent in compound **6** is replaced by an ethyl group. For compound **8**, the $\Delta G^{\neq}$ barrier of the inverse electron demand Diels-Alder reaction with the central tetrazine moiety was 41.02 kcal/mol, which was lower by 10.76 kcal/mol than that of the Diels-Alder reaction at the thiophene position (51.78 kcal/mol). Likewise for compound **9**, the $\Delta G^{\neq}$ barrier for Diels-Alder reaction with the tetrazine part is 35.74 kcal/mol, which is lower by 11.63 kcal/mol than that of the reaction between the furan moiety and compound **6**. The much higher $\Delta G^{\neq}$ of the normal Diels-Alder reaction on both the thiophene and furan moieties may in part justify the selectivity for the tetrazine moiety. Moreover, we cannot rule out the possibility that release of one nitrogen molecule during the inverse electron demand Diels-Alder reaction allows the reaction to move forward more favorably than taking a normal Diels-Alder reaction pathway with a higher energy barrier. Therefore it is rational that only inverse electron demand Diels-Alder reaction product was observed in real reactions. The frontier orbital energy level of compound **10** was investigated by cyclic voltammetry (Figure S18). The LUMO energy level obtained was -3.92 eV, which was about 0.26 eV lower than our previously reported electron deficient PPD monomer[17] and confirmed that the PAPD monomer is extremely electron deficient.[20] The single crystals of compounds **11** and **12** were obtained by slow vapor diffusion of methanol into their toluene solutions and the refined crystal structures confirmed the PAPD backbone structure (inserts in Scheme 1). Coupled with the ability for side chain engineering and the ease of incorporation of PAPD monomer into polymers, PAPD monomers are good candidates as electron acceptors for organic electronic polymers. Herein, a series of polymers using the PAPD monomer **10** was prepared. The random copolymers **P1** – **P5** were synthesized through Stille coupling polymerization[21] with different ratios of the electron acceptor **10**, 6,8-dibromo-3,3-bis((dodecyloxy)methyl)-3,4-dihydro-2*H*-thieno[3,4-*b*][1,4]dioxepine **13** and 2,5-bis(trimethylstannyl)thieno[3,2-b]thiophene **14** in a medium yield of 50-55% to demonstrate its influence on the optical properties and electrochromic performance. The polymers were purified by precipitation, followed by Soxhlet extraction with acetone, hexane and chloroform. The crude yields of polymers are typically above 85%. As these polymers have long straight and branched alkyl chains, polymers with low and moderate molecular weights are slightly soluble in acetone and hexane and therefore they could be gradually removed during the Soxhlet extraction process. Thus, the chloroform fraction contains high molecular weights polymers with a relatively low yield at ca. 50%. After our purification process, the obtained polymers typically have a Mn greater than 40,000g/mol. The chemical structures of the synthesized polymers are confirmed by ^{1}H NMR (Figure S9 – S13) and elemental analysis. Using polymer **P3** as an example, the signal at around 4.2 ppm corresponds to the N-CH_2 of the PAPD and a pair of O-CH_2 from two long alkoxy groups of the ProDOT moiety. The signal at around 3.6 ppm corresponds to the other 2 pairs of O-CH_2 from the seven membered-ring ProDOT unit. Polymer compositions were estimated by comparing the integration of these two characteristic peaks, and results are in good agreement with the reactant feed ratios. All the polymers exhibited high average-molecular weights (M_n) in the range of 42,000 – 67,000 g/mol and good thermal stability with decomposition temperatures at around 390 °C at 5 % weight loss under N_2 (Table 1). Differential scanning calorimetry revealed that no observable phase transition was observed for all five polymers (Figure S22) and XRD measurements confirmed that the polymers are amorphous (Figure S23). The bulky and branched alkyl chains attached on the rod-like conjugated polymers as well as random structure of the polymers may disturb the π-π conjugation and bring in amorphous natures[26].

3.2 Optical and electrochemical properties

The normalized UV-*vis* absorption spectra of polymers **P1 – P5** in chlorobenzene solutions and as thin films are shown in Figure 3a and the data are summarized in Table 2. All the polymers exhibited similar absorption spectra with absorptions that cover a range from 400 – 600 nm and their thin films exhibited spectral broadening and bathochromic shifts, suggesting the presence of aggregation in the solid state. With increasing amount of electron acceptors across **P1 – P5**, it is found that the polymers in the solution state reveal a systematic decrease in the absorption maximum from 535 to 500 nm. Similarly, the same trend is observed in the film state. This blue-shift in UV-vis absorbance may be due to the distorted planarity of the conjugated polymers. As the molar ratio of the PAPD unit increased, the steric hindrance of the branched side chain on the PAPD unit increased correspondingly, resulting in a

twisting of the backbone of the polymer chains and hence reduced the coplanarity. Similar observation in DA type polymers has also been reported by Reynolds's group[27]. Despite the differences in absorption maxima, the amount of electron acceptors in the polymer chain is observed to have insignificant influence on the bandgap of the polymers. The optical bandgaps (E_g^{opt}) of the polymers were determined from the onset of absorption of the thin films and were approximated to be 1.90 – 1.99 eV for polymers **P1** – **P5**. Cyclic voltammetry was conducted to analyze the electrochemical properties of polymers **P1** – **P5**. All five polymers exhibited quasi-reversible peaks and no reduction peak was observed in the *n*-doping region as shown in Figure 3b. The HOMO energy levels were estimated from the oxidation onset of the first peak and as more electron acceptor **10** was incorporated into the polymers (i.e., going from **P1** to **P5**), there is a gradual deepening of the HOMO energy level from -5.03 to -5.32 eV (Table 2). With deep HOMO energy levels, the polymers are expected to have better ambient stability.

3.3 Spectroelectrochemistry

The UV-*vis*-NIR spectra and color states of the sandwich devices of polymers **P1** – **P5** from the spectroelectrochemical analysis were shown in Figure 4 and 5. As mentioned earlier, the variations in absorption maxima of the polymers lead to discernible differences in the observed neutral-state colors, which coarsely transits from purple to red across polymers **P1** – **P5**. Upon progressive oxidation of the polymers by increasing the applied potential from 0.0 to 2.0 V, the absorption peak at the visible region depleted, and new absorption peaks appeared in the NIR region around 750 nm and 1230 nm representing the formation of polaronic and bipolaronic bands. For **P1** and **P2**, when potentials of 1.7 V or above are applied, the bipolaron bands intensity increased while the polaron bands were suppressed, and the spectra showed two clear isosbestic points at about 620 nm and 830 nm, which confirmed the presence of the interconverting neutral, polaronic and bipolaronic species. On the other hand, for **P3** – **P5**, only one isosbestic point was observed at ca. 600 nm, and this is due to the saturation of the polarons where these polarons are unable to convert to bipolarons despite the increased bias. Particularly for **P5**, there is reduced electroactivity as seen from the significantly small decrease in the intensity of the visible absorption (Figure 4e). As observed and discussed in our previous work,[22] saturation of the polaron species and the hindrance of the formation of the bipolaron species for **P3** – **P5** would possibly originate from the morphological variations and thin film quality of the polymers (*vide infra*). At the fully oxidized state (2.0 V), Polymer **P1** and **P2** reveals a residual tailing into the visible region. On the other hand, for **P3** – **P5**, an additional distinct peak is still apparent in the visible region. The peak at around 450 nm may be ascribed to the intrinsic color of the electron acceptor unit. Polymers **P1** – **P5** in their neutral states exhibit a purple/red color, which is reinforced by the very positive a* values between 32 – 41, but they show different hues as characterized by the considerably different b* values going from -18 to 24.[23] In their oxidized states, a* values for polymers **P1**–**P5** significantly decline from 32, 41, 34, 38 and 35 to -2, -1, 5, 8 and 19, associated with limited changes of b* values going from -18, -4, 2, 10 and 24 to -7, -4, 2, 8 and 20, respectively. As a result, polymer **P1** and **P2** shows a greyish blue and polymers **P3** and **P4** display a grey color when fully oxidized (Figure 5).

3.4 Electrochromic Performance

In order to study the electrochromic performance of polymers **P1** – **P5**, we evaluated the performance of these polymers using the fabricated absorption/transmission type devices. The optical contrasts, switching times and coloration efficiencies are summarized in Table 3. Optical contrast is calculated as the absolute difference in transmittance between oxidized and reduced states in a full switch, in which switching time corresponds to the time required for the polymer to reach 95 % of the full switch. In this work, the coloration efficiencies are calculated based on 95 % of the full switches. Electrochromic switching studies were carried out by switching the polymers between +1.6 V and -1.6V at 90 seconds interval and the plots are shown in Figure 6 and Figure S19. As seen from the spectroelectrochemical spectra shown above, when there are more electron acceptors being introduced in the polymer backbone, an increased residual absorption in the visible region of the charged species was observed. This is perhaps attributed to the increasing presence of highly electron-accepting groups, which reduce the polymer's propensity towards oxidation. Therefore, **P1** which does not contain any electron acceptor achieved the best optical contrast of 43.0 % at 540 nm. In particular for **P3**, it achieved a remarkable optical contrast of 80.5% in the near infrared (NIR) region. The coloration efficiencies at their λ_{max} were calculated to be 361, 212, 328, 239 and 156 cm^2/C for **P1 – P5** respectively, which are generally higher than that of the reported benchmark electrochromic polymer PEDOT (183 cm^2/C).[24]
Stability studies of ECDs were examined by monitoring the optical contrast as a function of the number of cycles. Potentials of + 1.6 V and - 1.6 V were applied with a full switch of 40 s. The redox reversibility of electrochromic polymers highly relies on the reactivity/stability of the radical cations (polarons) formed upon electrochemical oxidation. The stabilities of the ECDs were tested by subjecting the devices to repeated potential switching between + 1.6 V and - 1.6 V. Percent transmittance changes were monitored as a function of time at the infrared region at 1500 nm. The optical contrasts achieved by **P3** ECD at the initial and final stages of redox cycles are illustrated in Figure 7. The percentage transmittance dropped by 0.6% in contrast after 800 full cycles, implying that the polymer **P3** show very good redox stability. The polymers **P1**, **P2**, **P4** and **P5** showed relatively poorer performance in comparison with **P3** and results were given in Figure S20. The reason behind why the ECD perfomance of polymer **P3** is better than the rest of the polymers is not very clear and it is, however, beliveved that there is a rational or preferable ratio of electron acceptor in the whole D-A type conjugated polymer structure, and a too high (more than 30%) or low (less than 10%) electron acceptor ratio is not favourable to achieve high performance, in particular, long-term redox stability. More examples are required to verify the assumption mentioned above.

4. Conclusions

A unique PAPD building block with ultrahigh electron deficiency was synthesized through a region-selective inverse electron demand Diels-Alder reaction. We have demonstrated a series of D-A type conjugated polymers using the PAPD monomer. The PAPD-embedded polymers exhibited electrochromism and were able to switch between purple/red and blue/grey, and reveal good electrochromic properties such as high optical contrasts and very good redox stability. Facile side-chain engineering and convenient incorporation into D-A type conjugated polymers *via* palladium catalyzed cross coupling reaction, as well as characteristics with ultrahigh electron deficiency would render these new PAPD electron acceptors as promising candidates not only for electrochromic materials, but for organic photovoltaic solar cells and field effect transistors as well.[25]

Acknowledgements

The authors would like to thank the Agency for Science, Technology and Research (A*STAR) and Minister of National Development (MND) for their financial support (Grant no.: 1321760011). The TD-DFT calculations were supported by the A*STAR computational resource centre through the use of its high performance computing facilities.

References

1 (a) Y. -J. Cheng, S. -H. Yang and C. -S. Hsu, *Chem. Rev.,* 2009, **109**, 5868-5923; (b) P. Dutta, H. Park, W.-H. Lee, I. N. Kang and S.-H. Lee, *Polym. Chem.,* 2014, **5**, 132–143; (c) S. Guenes, H. Neugebauer and N. S. Sariciftci, *Chem. Rev.,* 2007, **107**, 1324-1338; (d) Z. Xiao, K. Sun, J. Subbiah, T. Qin, S. Lu, B. Purushothaman, D. J. Jones, A. B. Holmes and W. W. H. Wong, *Polym. Chem.,* 2015, **6**, 2312–2318; (e) N. Allard, N. Zindy, P.-O. Morin, M. M. Wienk, R. A. J. Janssen and M. Leclerc, *Polym. Chem.*, 2015, **6**, 3956-3961; (f) F. Grenier, R. B. Aïch, Y.-Y. Lai, M. Guérette, A. Holmes, Y. Tao, W. Wong and M. Leclerc, *Chem. Mater.*, 2015, **27**, 2137-2143.

2 (a) P. Deng and Q. Zhang, *Polym. Chem.,* 2014, **5**, 3298–3305; (b) Y. Li, P. Sonar, L. Murphy, and W. Hong, *Energy Environ. Sci.*, 2013, **6**, 1684. (c) X. Zhang, C. Xiao, A. Zhang, F. Yang, H. Dong, Z. Wang, X. Zhan, W. Li and W. Hu, *Polym. Chem.,* 2015, **6**, 4775–4783; (d) L. Biniek, B. C. Schroeder, C. B. Nielsen and I. *J.* McCulloch, *Mater. Chem.,* 2012, **22**, 14803-14813; (e) J.-R. Pouliot, B. Sun, M. Leduc, A. Najari, Y. Li and M. Leclerc, *Polym. Chem.*, 2015, **6**, 278-282.

3 (a) A. P. Kulkarni, C. J. Tonzola, A. Babel and S. A. Jenekhe, *Chem. Mater.,* 2004, **16**, 4556-4573; (b) Z. Yan, B. Sun, and Y. Li, *Chem. Commun.*, 2013, **49**, 3790-3792; (c) K. T. Kamtekar, A. P. Monkman and M. R. Bryce, *Adv. Mater.,* 2010, **22**, 572-582.

4 (a) H. -J. Yen and G. -S. Liou, *Polym. Chem.,* 2012, **3**, 255-264; (b) G. Sonmez, *Chem. Commun.,* 2005, 5251-5259; (c) K. Lin, S. Ming, S. Zhen, Y. Zhao, B. Lu and J. Xu, *Polym. Chem.,* 2015, **6**, 1487–1494; (d) W. T. Neo, L. M. Loo, J. Song, X, Wang, C. M. Cho, H. S. O. Chan, Y. Zong and J. Xu, *Polym. Chem.,* 2013, **4**, 4663–4675; (e) A. Bolduc and W. G. Skene, *Polym. Chem.,* 2014, **5**, 1119–1123; (f) B. Berns and B. Tieke, *Polym. Chem.,* 2015, **6**, 4887–4901; (e) B. Lu, S. Zhen, S. Zhang, J. Xu and G. Zhao, *Polym. Chem.,* 2014, **5**, 4896–4908.

5 (a) A. Kumar, D. M. Welsh, M. C. Morvant, F. Piroux, K. A. Abboud and J. R. Reynolds, *Chem. Mater.,* 1998, **10**, 896-902; (b) S. A. Sapp, G. A. Sotzing and J. R. Reynolds, *Chem. Mater.,* 1998, **10**, 2101-2108.

6 A. Balan, D. Baran, G. Gunbas, A. Durmus, F. Ozyurt and L. Toppare, *Chem. Commun.,* 2009, 6768-6770.

7 B. D. Reeves, C. R. G. Grenier, A. A. Argun, A. Cirpan, T. D. McCarley and J. R. Reynolds, *Macromolecules,* 2004, **37**, 7559-7569.

8 A. C. Arias, J. D. MacKenzie, I. McCulloch, J. Rivnay and A. Salleo, *Chem. Rev.,* 2010, **110**, 3-24.

9 A. A. Argun, P.-H. Aubert, B. C. Thompson, I. Schwendeman, C. L. Gaupp, J. Hwang, N. J. Pinto, D. B. Tanner, A. G. MacDiarmid and J. R. Reynolds, *Chem. Mater.,* 2004, **16**, 4401-4412.

10 F. C. Krebs, *Nat. Mater.,* 2008, **7**, 766-767.

11 J. Jensen, H. F. Dam, J. R. Reynolds, A. L. Dyer, and F. C. Krebs, *J. Polym. Sci. Part B: Polym. Phys.,* 2012, **50**, 536-545.

12 W. Cui and F. Wudl, *Macromolecules,* 2013, **46**, 7232-7238.

13 P. M. Beaujuge, C. M. Amb and J. R. Reynolds, *Acc. Chem. Res.,* 2010, **43**, 1396-1407.

14 (a) G. E. Gunbas, A. Durmus and L. Toppare, *Adv. Mater.,* 2008, **20**, 691-695; (b) P. M. Beaujuge, S. V. Vasilyeva, S. Ellinger, T. D. McCarley and J. R. Reynolds, *Macromolecules,* 2009, **42**, 3694-3706; (c) P. M. Beaujuge, S. Ellinger and J. R. Reynolds, *Adv. Mater.,* 2008, **20**, 2772-2776; (d) G. Sonmez, C. K. F.; Shen, Y.; Rubin and F. Wudl, *Angew. Chem. Int. Ed.,* 2004, **43**, 1498-1502; (e) G. Sonmez, H. B. Sonmez, C. K. F. Shen, R. W. Jost, Y. Rubin and F. Wudl, *Macromolecules,* 2005, **38**, 669-675.

15 (a) P. M. Beaujuge, S. Ellinger and J. R. Reynolds, *Nat. Mater.,* 2008, **7**, 795-799; (b) P. Shi, C. M. Amb, E. P. Knott, E. J. Thompson, D. Y. Liu, J. Mei, A. L. Dyer and J. R. Reynolds, *Adv. Mater.,* 2010, **22**, 4949-4953; (c) S. V. Vasilyeva, P. M. Beaujuge, S. Wang, J. E. Babiarz, V. W. Ballarotto and J. R. Reynolds, *ACS Appl. Mater. Interfaces,* 2011, **3**, 1022-1032.

16 M. İçli, M. Pamuk, F. Algi, A. M. Önal and A. Cihaner, *Chem. Mater.,* 2010, **22**, 4034-4044.

17 Q. Ye, W. T. Neo, C. M. Cho, S. W. Yang, T. Lin, H. Zhou, H. Yan, X. Lu, C. Chi and J. Xu, *Org. Lett.,* 2014, **16**, 6386-6389.

18 (a) R. Barattin and A. Gourdon, *Eur. J. Org. Chem.,* 2009, 1022-1026; (b) H. Herrera, P. de Echegaray, M. Urdanpilleta, M. J. Mancheno, E. Mena-Osteritz, P. Bauerle and J. L. Segura, *Chem. Commun.,* 2013, **49**, 713-715.

19 E. Kurach, D. Djurado, J. Rimarcik, A. Kornet, M. Wlostowski, V. Lukes, J. Pecaut, M. Zagorska and A. Pron, *Phys. Chem. Chem. Phys.,* 2011, **13**, 2690-2700.

20 K. Takimiya, I. Osaka and M. Nakano, *Chem. Mater.,* 2013, **26**, 587-593.

21 B. Carsten, F. He, H. J. Son, T. Xu and L. Yu, *Chem. Rev.,* 2011, **111**, 1493-1528.

22 Q. Ye, W. T. Neo, T. Lin, J. Song, H. Yan, H. Zhou, K. W. Shah, S. J. Chua and J. Xu, *Polym. Chem.,* 2015, **6,** 1487-1494.

23 *CIE Technical Report No. 15.2004, Colorimetry*, 3rd ed., CIE Central Bureau, Vienna, Austria 2004.

24 C. L. Gaupp, D. M. Welsh, R. D. Rauh and J. R. Reynolds, *Chem. Mater.,* 2002, **14**, 3964-3970.

25 (a) X. Guo, M. Baumgarten and K. Müllen, *Prog. Polym. Sci.,* 2013, **38**, 1832-1908; (b) X. Guo, A. Facchetti, and T. J. Marks, *Chem. Rev.,* 2014, **114**, 8943-9021. (c) A. Pron, M. Leclerc, *Prog. Polym. Sci.,* 2013, **38**, 1815-1831.

26 Mondal, R.; Bencerril, H. A.; Verploegen, E.; Kim, D.; Norton, J. E.; Ko, S.; Miyaki, N.; Lee, S.; Toney, M.F.; Brédas, J. L.; Bao, Z., *J. Mater. Chem.*, 2010, **20**, 5823-5834.

27 Steckler, T. T.; Abboud, K. A.; Craps, M.; Rinzler, A. G.; Reynolds, J. R., *Chem. Commun.*, 2007, 4904-4906.

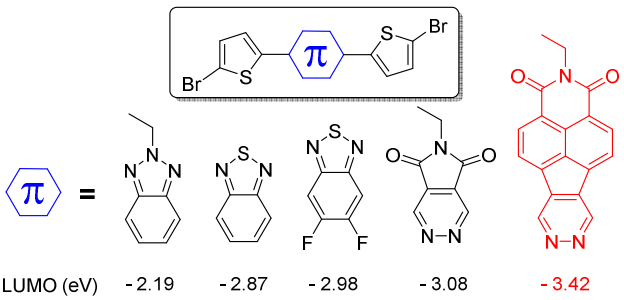

Figure 1 Calculated LUMO energy levels of a series of electron acceptors. The identities of the electron acceptor moiety from left to right: benzotriazole, benzothiadiazole, 5,6-difluorobenzo[1,2,5]thiadiazole, pyrrolo[3,4-*d*]pyridazine-5,7-dione and a PAPD monomer.

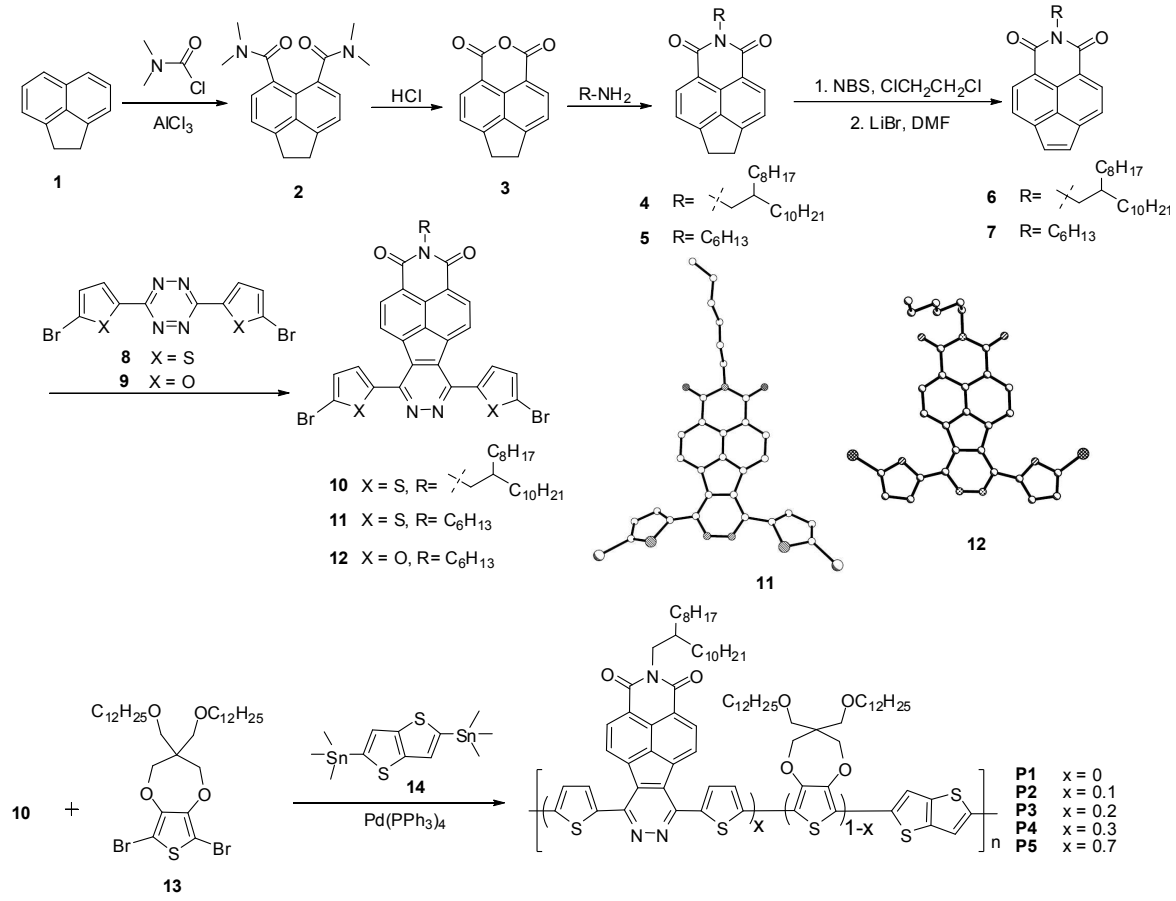

Scheme 1 Synthetic routes leading to PAPD monomers **10** – **12** and polymers **P1** – **P5**. Inserts: single crystal structures of compounds **11** and **12**; Hydrogen atoms are omitted for clarity.

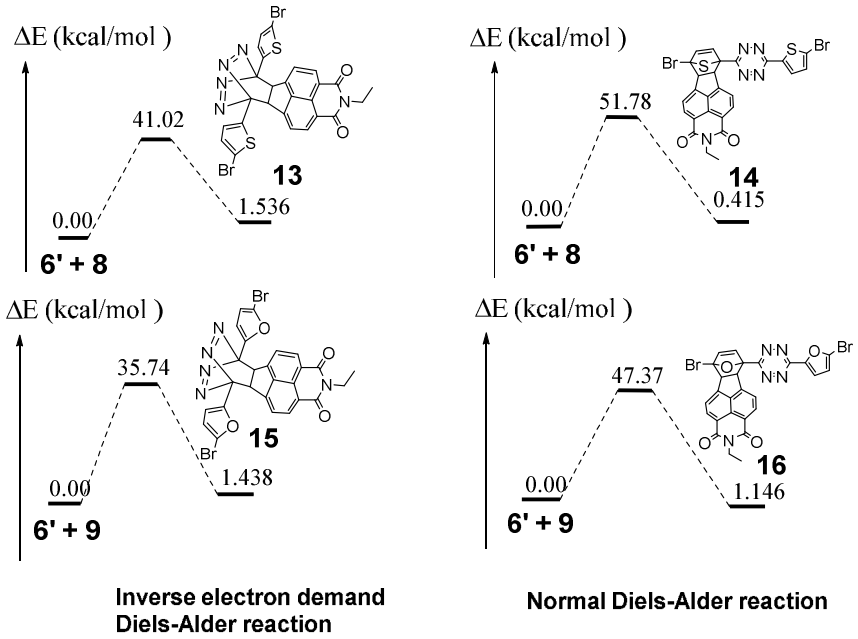

Figure 2 Gibbs free energy profiles of normal Diels-Alder reaction and inverse electron demand Diels-Alder reaction pathways to attach compound **6'** onto compounds **8** and **9**. Gibbs free energies are expressed in kcal/mol. Compound **6'** is chosen to replace compound **6** in order to avoid complexity of computation of compound **6** with a large branched side chain.

Table 1 Synthetic yields, molecular weights, polydispersity indexes and thermal decomposition temperatures of polymers **P1 – P5**.

Polymer	Yields (%)	M_n (g/mol)	M_w (g/mol)	PDI	T_D (°C)
P1	55	50,500	94,200	1.86	354
P2	55	42,100	83,500	1.98	389
P3	50	48,300	73,400	1.52	389
P4	54	54,500	93,800	1.72	398
P5	52	67,200	114,700	1.71	398

M_n: the number average molecular weight. M_w: the weight average molecular weight. PDI: polydispersity index. T_D: decomposition temperature at 5 % weight loss in N_2.

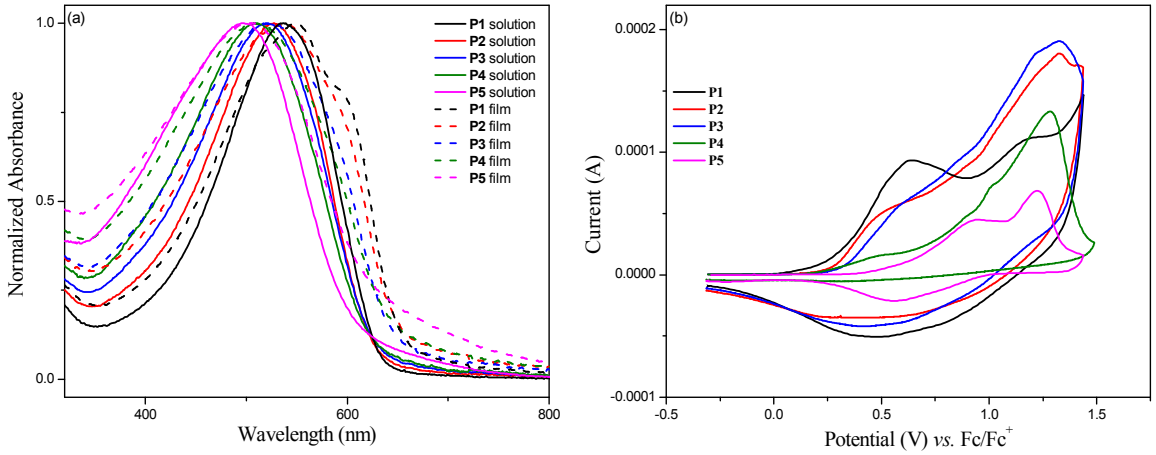

Figure 3 (a) Normalized UV-*vis* absorption spectra of **P1 – P5** in chlorobenzene and in thin film state. (b) Cyclic voltammograms of **P1 – P5** thin films in a 0.1M $LiClO_4$/ACN electrolyte/solvent couple at a scan rate of 50 mV·s^{-1} calibrated against the ferrocene/ferrocenium couple.

Table 2 Summary of optical and electrochemical properties of polymers **P1 – P5** in solution and in film state.

	In solution		In film state		$^aE_g^{opt}$ (eV)	^bHOMO (eV)	^cLUMO (eV)
	λ_{max} (nm)	λ_{onset} (nm)	λ_{max} (nm)	λ_{onset} (nm)			
P1	535	629	550	651	1.90	-5.03	-3.13
P2	528	622	540	646	1.92	-5.07	-3.15
P3	519	623	522	640	1.94	-5.11	-3.17
P4	510	624	510	640	1.94	-5.21	-3.27
P5	500	604	505	622	1.99	-5.32	-3.33

$^aE_g^{opt}$ is calculated following the equation $E_g^{opt} = 1240/\lambda_{onset}$ (eV); $^bE_{HOMO} = -(E_{onset,ox}$ vs ferrocene) – 4.8; $^cE_{LUMO} = E_{HOMO} + E_g^{opt}$

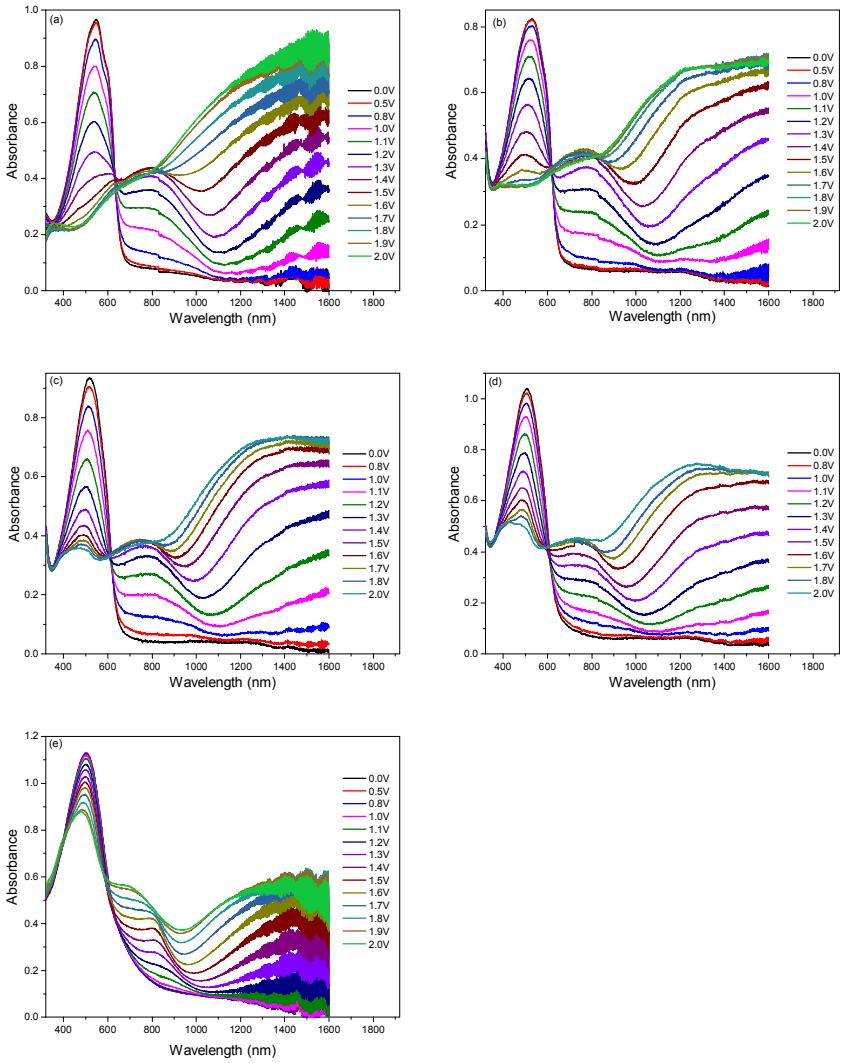

Figure 4 Spectroelectrochemistry of (a) **P1**, (b) **P2**, (c) **P3**, (d) **P4** and (e) **P5** at various applied potentials.

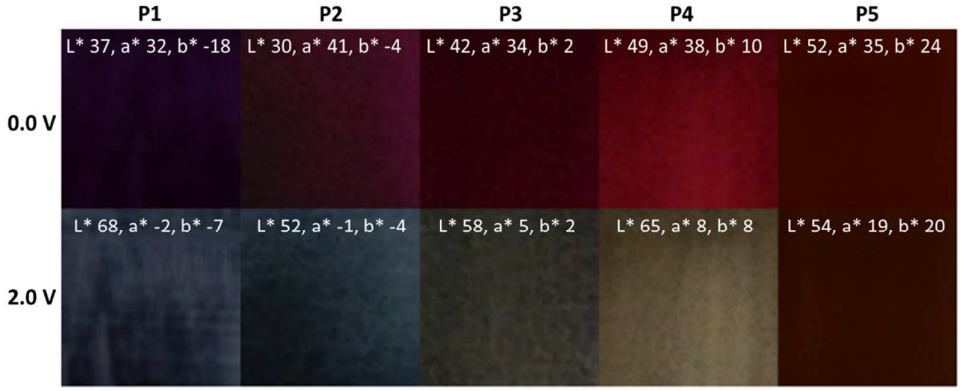

Figure 5 Color states of **P1** – **P5** at 0.0 V (purple/red) and 2.0 V (blue/grey) with L* a* b* values.

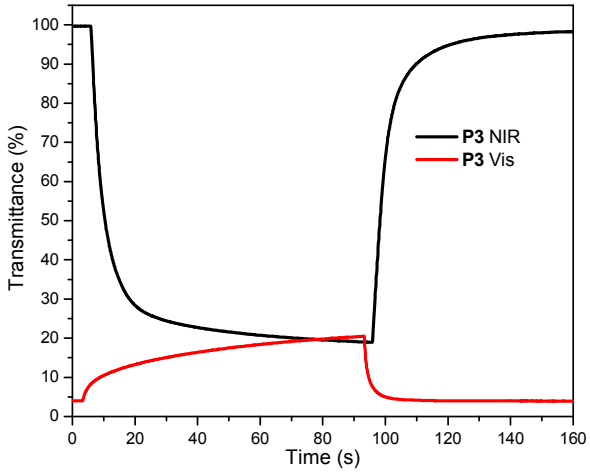

Figure 6 Square-wave potential step absorptiometry of polymer **P3** device in the visible and NIR regions.

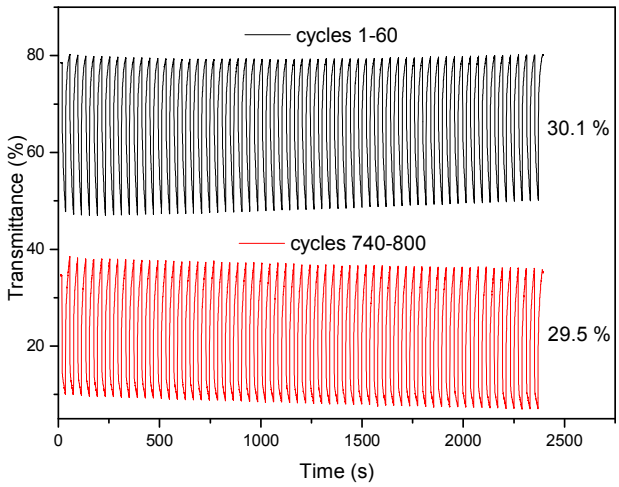

Figure 7 Stability testing of **P3** ECD through square-wave potential step absorptiometry monitored at 1500 nm between 1.6 V and -1.6 V with a switch time of 40 s. The transmittance for graphs is offset for clarity and it does not reflect the actual transmittance values. Measurements were carried out after 100-cycle equilibrium under ambient conditions. The device was not encapsulated.

Table 3 Performance of electrochromic device of polymers **P1 – P5**[a].

	Visible (λ_{max})				NIR (1500 nm)			
	Contrast (%)	Bleaching (s)	Coloration (s)	CE (cm^2/C)	Contrast (%)	Bleaching (s)	Coloration (s)	CE (cm^2/C)
P1	43.0	55.0	10.0	361	78.6	14.5	38.7	353
P2	32.1	50.4	5.5	212	59.5	12.4	29.2	300
P3	16.4	73.7	8.2	328	80.5	22.5	31.6	368
P4	15.5	59.8	4.9	239	66.1	17.3	54.8	394
P5	2.0	71.5	9.7	156	54.0	30.8	68.6	46.4

[a]The bleaching time is defined as the time required for an ECD to change from its coloured to bleached state. In our studies the bleaching time is defined as the time required for increase of the transmittance to 95% of the transmittance difference between the coloured and bleached states. The coloration time is defined as the time required for an ECD to change from its bleached to coloured state. In our studies the coloration time is defined as the time required for reduction of the transmittance to 95% of the transmittance difference between the bleached and coloured states.

Graphical abstract

Ultrahighly Electron-Deficient Pyrrolo-acenaphtho-pyridazine-dione Based Donor-Acceptor Conjugated Polymers for Electrochromic Applications

ChingMui Cho,[†,#,‡] Qun Ye,[†,‡] Wei Teng Neo,[†,‖] Tingting Lin,[†] Xuehong Lu,[#,*] and Jianwei Xu[†,§,*]

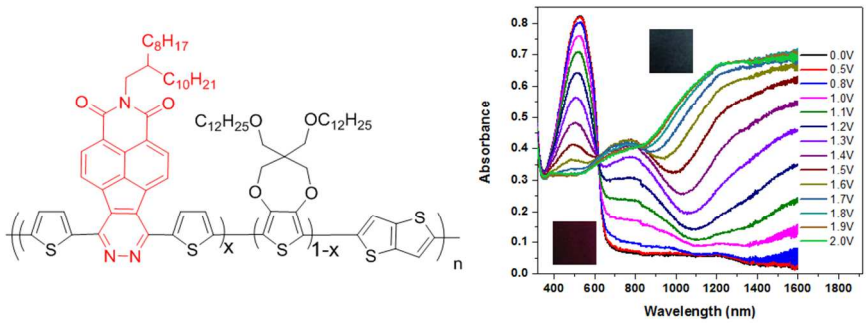

New ultrahighly electron-deficient acceptors pyrrolo-acenaphtho-pyridazine-diones (PAPD) was synthesized via a region-selective inverse electron demand Diels-Alder reaction and their corresponding conjugated polymers showed electrochromism with long-term stability.